RESEARCH ARTICLE

The protocadherin alpha cluster is required for axon extension and myelination in the developing central nervous system

Wen-cheng Lu[1], Yu-xiao Zhou[2], Ping Qiao[3], Jin Zheng[2], Qiang Wu[2,*], Qiang Shen[1,*]

1 Department of Orthopedics, Shanghai General Hospital, Shanghai Jiao Tong University School of Medicine, Shanghai, China

2 Center for Comparative Biomedicine, Key Laboratory of Systems Biomedicine (Ministry of Education), Institute of Systems Biomedicine, Shanghai Center for Systems Biomedicine, Shanghai Jiao Tong University, Shanghai, China

3 Department of Orthopedics, People's Hospital of Zhangqiu, Zhangqiu, Shandong Province, China

Funding: *This study was supported by a grant from the Science and Technology Commission of Shanghai Municipality of China, No. 12441900702.*

Graphical Abstract

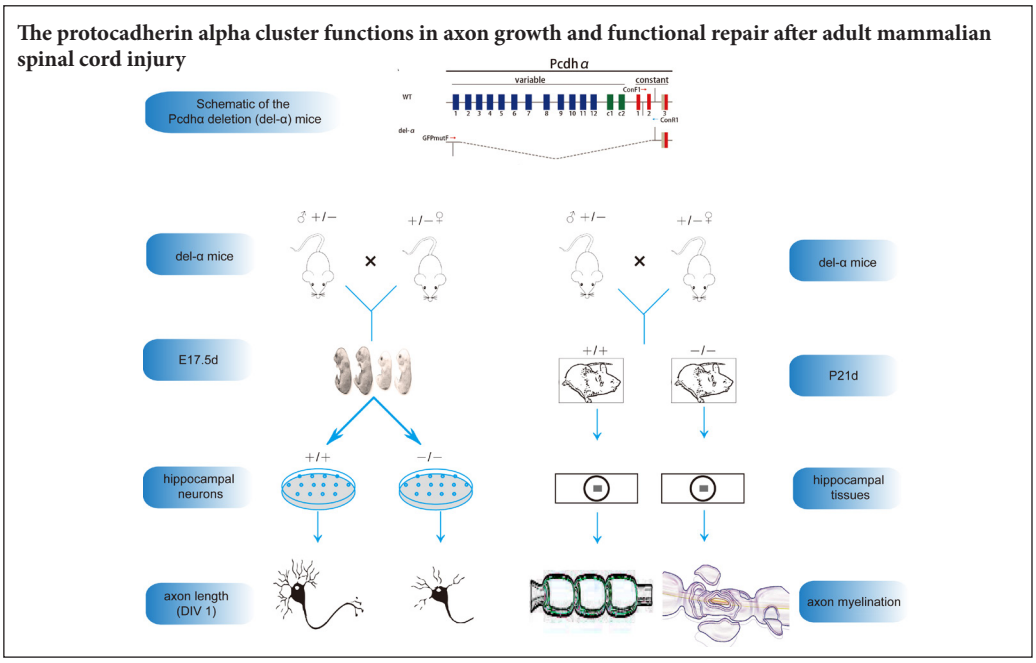

***Correspondence to:**
Qiang Wu, Ph.D. or Qiang Shen, M.D., Ph.D., qwu123@gmail.com or shmail1231@yahoo.com.

orcid:
0000-0002-7782-9963 (Qiang Shen)

doi: *10.4103/1673-5374.228724*

Accepted: *2018-01-12*

Abstract

In adult mammals, axon regeneration after central nervous system injury is very poor, resulting in persistent functional loss. Enhancing the ability of axonal outgrowth may be a potential treatment strategy because mature neurons of the adult central nervous system may retain the intrinsic ability to regrow axons after injury. The protocadherin (Pcdh) clusters are thought to function in neuronal morphogenesis and in the assembly of neural circuitry in the brain. We cultured primary hippocampal neurons from E17.5 Pcdhα deletion (del-α) mouse embryos. After culture for 1 day, axon length was obviously shorter in del-α neurons compared with wild-type neurons. RNA sequencing of hippocampal E17.5 RNA showed that expression levels of BDNF, Fmod, Nrp2, OGN, and Sema3d, which are associated with axon extension, were significantly down-regulated in the absence of the Pcdhα gene cluster. Using transmission electron microscopy, the ratio of myelinated nerve fibers in the axons of del-α hippocampal neurons was significantly decreased; myelin sheaths of P21 Pcdhα-del mice showed lamellar disorder, discrete appearance, and vacuoles. These results indicate that the Pcdhα cluster can promote the growth and myelination of axons in the neurodevelopmental stage.

Key Words: *nerve regeneration; spinal cord injury; axons; protocadherin α cluster; hippocampal neurons; RNA sequencing; real-time quantitative polymerase chain reaction; transmission electron microscopy; neural regeneration*

Introduction

During neuronal wiring, axons establish a framework that is dependent on a series of guidance events during neural development. Axon outgrowth is crucial for the assembly of neuronal circuitry to ensure proper synaptic connectivity (Dickson, 2002; Chilton, 2006; McAllister, 2007; Imai et al., 2009; Cheng and Poo, 2012). Meanwhile, myelin is an important structure in the nervous system. Myelin alteration or myelination cell dysfunction affects the function of axons, including outgrowth of axons during development (Sánchez

et al., 1996). Axon regeneration after injury requires axonal outgrowth from the soma, similar to that during normal development. Injured axons in the adult mammalian spinal cord ordinarily fail to spontaneously regenerate and do not recover functionality. Axon demyelination further increases the difficulty of regeneration after injury (Xu et al., 2014; Kim et al., 2017). A number of factors are thought to be responsible for this phenomenon, including extracellular matrix inhibitors, myelin inhibition, cell death, insufficient growth factor support, and the lack of the intrinsic growth capacity of adult central nervous system neurons (Beattie et al., 2000; Neumann et al., 2002; Filbin, 2003; Fawcett, 2006; Liu et al., 2011; McKerracher and Rosen, 2015).

Many researchers have tried to characterize the environmental inhibitory molecules in the adult central nervous system (Hu and Selzer, 2017; Nathan and Li, 2017). However, removing the inhibitory molecules genetically or pharmacologically only results in limited sprouting and is insufficient for long-distance axon regeneration (Yiu and He, 2006; Filbin, 2008; Fitch and Silver, 2008; Yang et al., 2010). Many studies have attempted to explore the intrinsic regenerative ability of mature central nervous system neurons to promote axon regeneration (Kadoya et al., 2009; Sun and He, 2010; Yang and Yang, 2012). Intrinsic growth activity is gradually repressed in the transition process from embryonic to adult neurons (Abe and Cavalli, 2008; Lu et al., 2014). Thus, an important step in elucidating the mechanisms mediating this activity is to identify the critical genes that promote neurite outgrowth.

Protocadherins (Pcdhs) are a large group of calcium-binding transmembrane cell-adhesion and signaling proteins, belong to the cadherin superfamily, and are subgrouped into "clustered" and "non-clustered" Pcdhs based on their respective genomic structures (Yagi and Takeichi, 2000; Morishita and Yagi, 2007; Kim et al., 2011; Hayashi and Takeichi, 2015). In mammals, more than 50 clustered *Pcdh* genes are organized into three sequentially-linked clusters known as *Pcdhα*, *Pcdhβ*, and *Pcdhγ* (Wu and Maniatis, 1999; Wu et al., 2001). The clustered *Pcdh* genes are expanded in species with rich behavior repertoires such as zebrafish and octopus but not in *Drosophila* (Wu et al., 2001; Albertin et al., 2015). Some non-clustered protocadherins, such as Pcdh-17, Pcdh18b, and NF-Pcdh, participate in axon extension and arborization (Biswas et al., 2014; Hayashi et al., 2014; Leung et al., 2015). Recent studies have indicated that mice with complete deletion of the *Pcdhα* cluster or its constant region are viable and fertile, although they exhibit abnormal axonal projections from olfactory sensory neurons, defects in dendritic branching, and altered spine morphogenesis and oligodendrocyte development (Hasegawa et al., 2008; Hasegawa et al., 2012; Suo et al., 2012; Yu et al., 2012). Furthermore, Pcdhα may function in the establishment and maintenance of appropriate synaptic connections (Zipursky and Sanes, 2010; Chen and Maniatis, 2013). We predicted that the *Pcdhα* cluster may be key in the outgrowth of axons because of these characteristics.

This study investigated the molecular functions of the Pcdhα cluster, focusing on its relationship with axon growth and myelination. The aim of this study was to investigate the axon growth defects and myelin sheath deficiency in hippocampal neurons of *Pcdhα* knockout mice.

Materials and Methods

Animals

Pcdhα knockout (Pcdhα-del) mice were prepared previously (Wu et al., 2007, 2008) and housed in the Experimental Animal Center of Shanghai Jiao Tong University of China. Mice were able to reproduce. Male and female mice aged approximately 3 months were used (Animal use license No. SYXK (Hu) 2013-0052). Animals were maintained at 23.8°C under a 12-hour light/dark cycle (lights on from 07:00–19:00). All experiments complied with the guidelines of the Institutional Animal Care and Use Committee of Shanghai Jiao Tong University (approval No. 1602029).

Mice genotyping

DNA extraction from tail biopsies and genotyping was performed according to a previous study (Truett et al., 2000). Primers used were as follows: ConF1: 5′-AGG CTG AAT AAC GTG CAC AGC TAA G-3′; GFPmutF: 5′-CCC CCT GAA CCT GAA ACA TAA AAT G-3′; ConR1: 5′-GCA GAT TGG TTC AAT GGA GTC TTT-3′.

Hippocampal neuron culture

Heterozygous Pcdhα-del female mice were crossed with heterozygous Pcdhα-del male mice. Embryonic day 17.5 (E17.5) embryos were collected from a pregnant dam and genotyped. Wild-type and Pcdhα-del embryos were prepared for neuronal culture. Hippocampi were collected in Hanks' Balanced Salt Solution containing 10 mM Hepes (Gibco, Grand Island, NY, USA), 0.5% glucose and 100 μg/mL penicillin/streptomycin. Tissues were digested with 0.25% trypsin for 15 minutes at 37°C. After terminating the reaction with trypsin inhibitor (0.5 mg/mL) for 3 minutes at room temperature, tissues were gently triturated in the plating medium, containing minimum essential medium (Gibco, Grand island, NY, USA), 10% fetal bovine serum (Gibco), 1 mM glutamine (Sigma, St. Louis, MO, USA), 10 mM Hepes (Gibco), and 50 μg/mL penicillin/streptomycin (Gibco). The number of viable cells was counted using 0.4% trypan blue in a hemocytometer (QIUJING, Shanghai, China). Cells were plated at a density of 1,000 cells/mm^2 on poly-L-lysine/Laminin coated coverslips (Becton, Dickinson, and Company BD Corning, Corning, NY, USA) in 24-well culture dishes (Thermo, Waltham, MA, USA). Cells were incubated in an atmosphere of 5% CO_2 at 37°C. After 3–4 hours, the plating medium was replaced with a serum-free culture medium, supplemented with neurobasal medium (Gibco), 2% B27, 0.5 mM glutamine, 50 mg/mL penicillin/streptomycin, and 25 mM glutamate (Sigma).

Immunofluorescent staining

Cultured primary hippocampal neurons were washed once with 1× PBS, and then fixed in 4% paraformaldehyde for 20 minutes at room temperature. Neurons were permeabi-

lized and blocked with 0.3% Triton X-100 and 5% bovine serum albumin for 10 minutes, followed by incubation with mouse anti-Tau-1 primary antibody (monoclonal, 1:5,000; Millipore, Billerica, MA, USA) at 4°C overnight and then with a secondary antibody, donkey anti-mouse IgG (1:5,000; Jackson ImmunoResearch, West Grove, PA, USA). F-actin was stained with rhodamine phalloidin (Thermo) at 4°C overnight. Cell nuclei were visualized with 4′,6-diamidino-2-phenylindole (DAPI). Images were collected with a Nikon confocal microscope (Tokyo, Japan) (A1Si) under a 20× objective for axon analysis. For each mouse embryo, nine fields of vision were randomly selected and pictures taken. The neuronal culture and immunofluorescent staining were performed at least three times.

RNA sequencing of hippocampal tissues

Hippocampal tissue was collected from E17.5 embryos according to the above-mentioned method. Three wild-type embryos and three Pcdhα-del embryos were prepared for RNA sequencing. Total RNA was prepared from embryonic hippocampal tissue using TRIzol Reagent (Ambion, Austin, TX, USA) according to the manufacturer's protocol. The quality and yield of the isolated RNA were assessed using a microplate reader and 1% agarose gel electrophoresis. Prior to synthesizing cDNA, 2 μg RNA was purified using oligo (dT) magnetic beads. ProtoScript II reverse transcriptase and random primers (Promega, Madison, WI, USA) were used for reverse transcription, and second-strand cDNA synthesis was then performed. The polymerase chain reaction (PCR) product was purified using AMPure XP beads. Total cDNA was used to prepare the sequencing library according to the method outlined in the NEBNext Ultra RNA Library Prep Kit for Illumina (NEB E7530, Beverly, MA, USA). The cDNA libraries were sequenced on an Illumina instrument with 50-base pair single reads. The read was aligned to the mouse genome (National Center for Biotechnology Information) using TopHat and Bowtie, followed by Cufflinks for assembly of the reads into transcripts. Relative abundance of transcripts was measured by Fragments Per Kilobase of exon per Million mapped fragments. The mapping of sequence data to the genome and transcriptome was visualized in Integrative Genomics Viewer, and genes with a maximum *P*-value of 0.05 and a minimum fold change of ±2 were selected as differentially expressed genes. GO terms were assigned to genes with significant differences in expression according to Gene Ontology.

Real-time quantitative polymerase chain reaction (RT-qPCR)

Hippocampi from E17.5 embryos were collected according to the above-mentioned method. Tissues were homogenized and lysed in TRIzol reagent according to the manufacturer's protocol (Life Technology). RNA yields were measured using a NanoDrop 2000 (Thermo, Waltham, MA, USA). A reverse transcription system (Promega) was used to obtain cDNA. Real-time PCR was performed on an Applied Biosystems real-time system according to the detailed instructions provided by FastStart Universal SYBR Green Master (Roche, Basel, Switzerland). For normalization of gene expression, glyceraldehyde-3-phosphate dehydrogenase (GAPDH) was used as an internal standard. Primers used are listed in **Table 1**.

Table 1 Sequences of primers used in real-time quantitative polymerase chain reactions

Primer	Sequence (5'–3')
Nrp2	F: GAC TTC ATT GAG ATT CGG GAT GG
	R: AAC TTG ATG TAT AAC ACG GAG CC
Sema3d	F: GGA AAA GCG ACA AGA GTT GC
	R: TGA AAA TTT TGT TTT TCA AAC ACT G
BDNF	F: CAG GTG AGA AGA GTG ATG ACC
	R: ATT CAC GCT CTC CAG AGT CCC
FMOD	F: TGA AGG GTT GTT ACG CAA ATG G
	R: GCA TAA GGC GGA CTG CAT AGT G
OGN	F: TGC TTT GTG GTC ACA TGG AT
	R: GAA GCT GCA CAC AGC ACA AT
GAPDH	F: GGT GAA GGT CGG TGT GAA CG
	R: CTC GCT CCT GGA AGA TGG TG

GAPDH: Glyceraldehyde-3-phosphate dehydrogenase; F: forward; R: reverse.

Transmission electron microscopy

Twenty-one days after birth is the peak time for myelin basic protein expression in the myelin sheath of the central nervous system, *i.e.*, the critical period of myelination. Therefore, myelin was observed at this time using electron microscopy (Sánchez et al., 1996). Three postnatal 21-day male wild-type mice and three postnatal 21-day male Pcdhα-del mice were prepared for transmission electron microscopy. Hippocampi were fixed overnight with 2.5% glutaraldehyde in 0.1 M sodium phosphate buffer, pH 7.4. Tissues were then washed with 0.1 M sodium phosphate buffer and post-fixed in 1% osmium tetroxide. Tissues were dehydrated in a graded series of ethanol and then embedded in resin. Several semi-thin sections were cut for anatomical orientation under light microscopy before ultrathin sectioning. The samples were ultrathin sectioned and then examined using a transmission electron microscope (Philips CM-120, Amsterdam, The Netherlands).

Data analysis

Statistical analysis was performed using GraphPad Prism5 software (Version X; La Jolla, CA, USA). The axon of each neuron was traced using ImageJ software (NIH, Bethesda, MD, USA). The resulting trace was used to calculate the length. The calculation was carried out in a double-blind fashion with respect to homozygous Pcdhα-del and wild-type littermates. For RT-qPCR, each sample was tested in triplicate and relative gene expression was calculated using the formula $2^{-\Delta\Delta Ct}$. Percentages of myelinated axons were checked manually. The results were taken in double-blind fashion with respect to homozygous Pcdhα-del and wild-type genotypes. All data were analyzed by two-tailed Student's *t*-test to assess the significance of difference from controls.

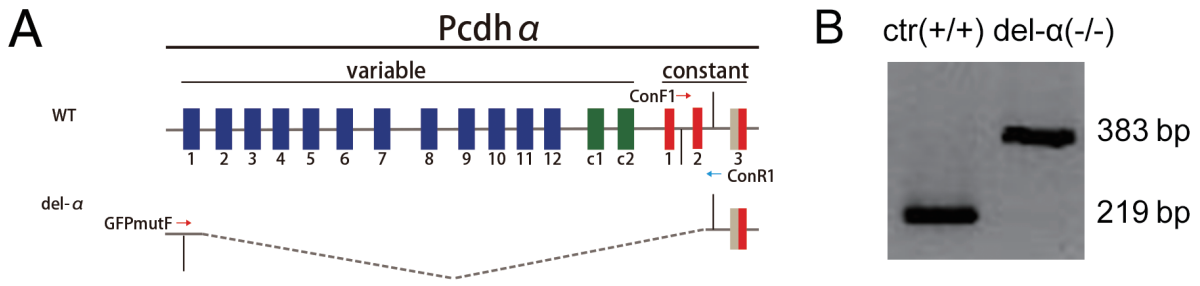

Figure 1 Genotyping of mice with deletion of the entire *Pcdhα* gene cluster.
(A) Schematic representation of del-α mice. (B) Genotyping of the *Pcdh* cluster knockout by polymerase chain reaction. In wild-type mice, conF1 and conR1 primers can produce a 219-bp fragment. Forward primer GFPmutF is not involved in PCR at this time. There is a long distance from reverse primer conR1. In gene knockout mice, GFPmutF and conR1 primers can produce a 383-bp fragment. At this time, the site to which the forward primer ConF1 binds has been knocked out and is not involved in PCR. Ctr: Control; del-α: Pcdhα deletion.

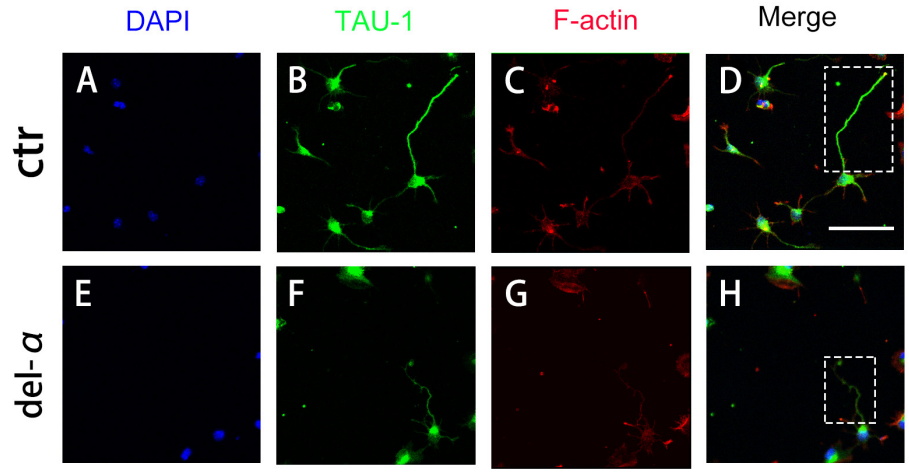

Figure 2 The *Pcdhα* gene cluster is required for axonal growth in cultured hippocampal neurons.
All neurons were visualized by staining with DAPI (blue) (A, E), and anti-Tau-1 (green) (B, F). Tau-1 was used as a marker for axons whose immunofluorescence is distributed in somas and axons. Actin was detected with rhodamine phalloidin (red) (C, G) and merged images are shown in D and H. Representative images of hippocampal neurons from control (A–D) and del-α (E–H) mice cultured for 1 day *in vitro*. Axons are represented in the dotted box in D and H. The neuronal culture and immunofluorescent staining were performed at least three times. Scale bar: 10 μm. DAPI: 4′,6-Diamidino-2-phenylindole; Ctrl: control; del-α: Pcdhα deletion.

Results

Axon growth defects in cultured *Pcdhα*-del neurons

To compare axonal growth changes between Pcdhα-del and wild-type mouse neurons, we observed cultured hippocampal neurons in a 24-hour period by confocal microscopy through immunofluorescence staining. Mice were genotyped by PCR before hippocampi were collected (**Figure 1**). Cells were seeded on coverslips coated with poly-L-lysine/laminin and cultured. The morphology of neurons was diverse and neurite outgrowth was remarkable after 24 hours. Cells were stained with DAPI (**Figure 2A, E**). There was no difference in nuclei morphology. Tau is a microtubule binding protein that stabilizes microtubules in growing axons. An anti-Tau-1 antibody was used to stain the axon, cell bodies, and dendrites of growing hippocampal neurons. The morphology of neurons was identified *via* Tau-1 staining. A neuron had one axon and multiple dendrites. The axon was always thin and funicular. We found that axon length was significantly decreased in Pcdhα mutants compared with controls (**Figure 2B, F**). This indicates that the *Pcdhα* cluster may function in axon outgrowth in cultured hippocampal neurons. Microfilaments consisting of actin, are widely distributed in neuronal soma and neurites, and can adapt to the physiological activities of neurons with morphological changes. Rhodamine phalloidin was used to stain F-actin, to show the integrity of the neurons (**Figure 2C, G**). These *in vitro* data suggest a potential role of the *Pcdhα* cluster in axon development *in vivo*.

Loss of Pcdhα resulted in axon length shortening in cultured hippocampal neurons

To further determine the role of clustered Pcdhs in axonal outgrowth, ImageJ software was used to analyze the length of axons. The axon length of wild-type neurons was 13.75 ± 0.95 μm after *in vitro* culture for one day. In contrast axon length in Pcdhα-del neurons was 10.85 ± 0.50 μm ($P < 0.05$, *vs.* control group; **Figure 3**). These data confirmed that the *Pcdhα* genes play an important role in axonal development.

Pcdhα mutants affected transcriptional levels of genes related to multiple axonal activities

To determine changes in transcription of genes related to axon growth and extension in Pcdhα-del mice, we compared hippocampal transcriptome profiles between wild-type and Pcdhα-del mice using next-generation RNA sequencing. According to a cutoff threshold of > 2 fold change and P value < 0.05, 1,341 RNA transcripts were identified, of which1,125 were downregulated and 216 upregulated (**Figure 4A**) in Pcdhα-del mice. According to GO analysis, these differentially expressed transcripts are enriched for several cellular components that are crucial in several biological processes, including axon extension, axon guidance and spinal cord development (**Figure 4B** and **Table 2**). A group of prom-

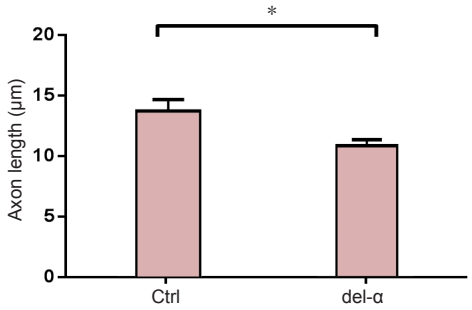

Figure 3 Effect of Pcdhα loss on axon length in cultured hippocampal neurons.
Data are expressed as the mean ± SD. Ctrl (+/+) is 13.75 ± 0.95 (μm) (n = 45). del-α (−/−) is 10.85 ± 0.50 (μm) (n = 35). *P < 0.05 (two-tailed Student's t-test). Ctrl: Control; del-α: Pcdhα deletion.

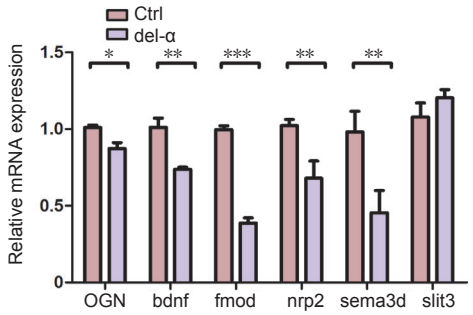

Figure 5 Validation of axonal extension gene expression in the hippocampus of E17.5 mice using real-time quantitative polymerase chain reactions.
Data are expressed as the mean ± SD. *P < 0.05, **P < 0.01, ***P < 0.001 (two-tailed Student's t-test). Ctrl: Control; del-α: Pcdhα deletion.

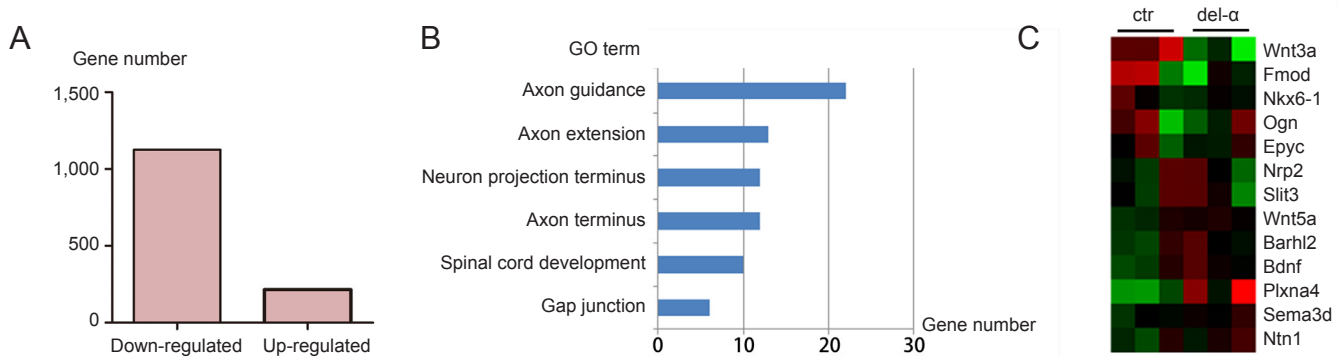

Figure 4 Transcriptional program in the hippocampus of E17.5 mice in the Ctrl (+/+) and del-α (−/−) groups.
(A) Genes differentially expressed in the hippocampus of controls and Pcdhα-del mice. (B) GO terms of neural development and axonal extension. (C) The expression of GO term 'axon extension' genes; red for high expression and green for low expression. Ctrl: Control; del-α: Pcdhα deletion.

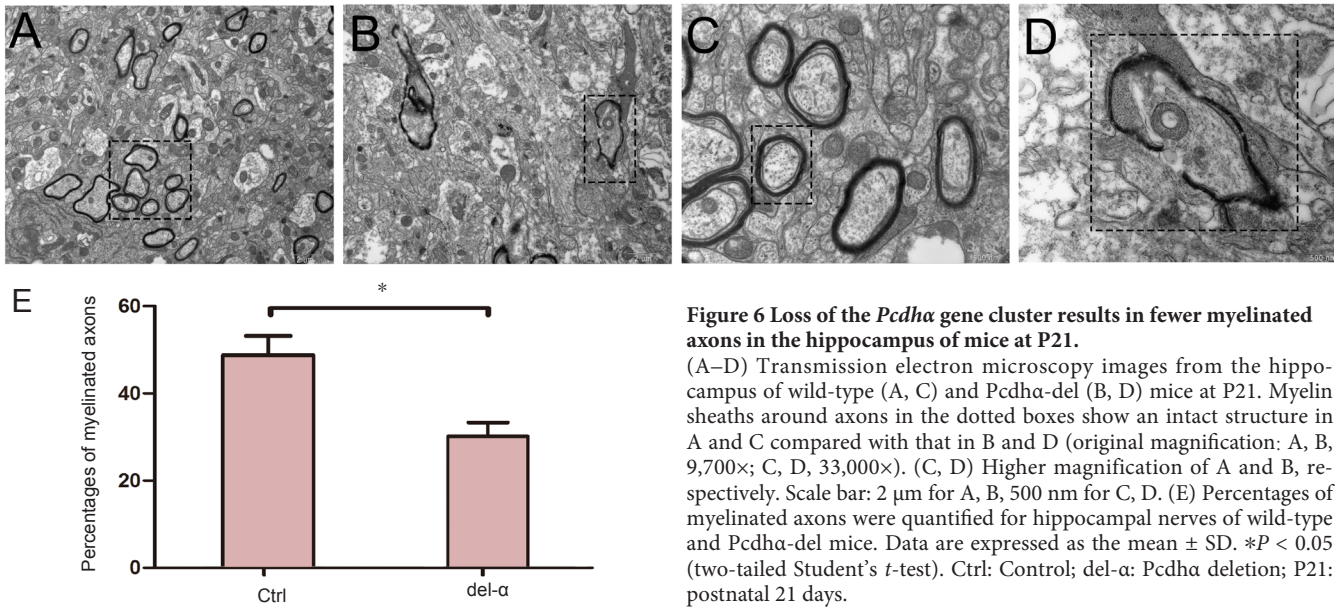

Figure 6 Loss of the *Pcdhα* gene cluster results in fewer myelinated axons in the hippocampus of mice at P21.
(A–D) Transmission electron microscopy images from the hippocampus of wild-type (A, C) and Pcdhα-del (B, D) mice at P21. Myelin sheaths around axons in the dotted boxes show an intact structure in A and C compared with that in B and D (original magnification: A, B, 9,700×; C, D, 33,000×). (C, D) Higher magnification of A and B, respectively. Scale bar: 2 μm for A, B, 500 nm for C, D. (E) Percentages of myelinated axons were quantified for hippocampal nerves of wild-type and Pcdhα-del mice. Data are expressed as the mean ± SD. *P < 0.05 (two-tailed Student's t-test). Ctrl: Control; del-α: Pcdhα deletion; P21: postnatal 21 days.

inent neuronal activity-regulated genes, including BDNF, Fmod, Nrp2, OGN, and Sema3d, was down-regulated in the hippocampus in the absence of Pcdhα (**Figure 4C**).

RT-qPCR verification of the transcriptome sequencing results

To validate the reliability of the deep sequencing data, we confirmed the alteration of expression using RT-qPCR. Six significantly differentially expressed genes in the GO term axon extension were selected. As shown in **Figure 5**, the expression pattern of these five genes was in concordance with the deep sequencing results. Among the six genes, the expression of Slit3 was up-regulated, while the other genes, including BDNF, Fmod, Nrp2, OGN, and Sema3d, were down-regulated.

Table 2 Genes in GO terms related to neural development and axonal extension

GO term	GO category	Symbols in list
Gap junction	Cellular component	Gja1, Calb2, Gjb2, Nov, Gjb6, Gja5
Axon terminus	Cellular component	Ntsr1, Th, Slc17a8, Ccl2, Casr, Calb2, Cdh1, Calca, Chrm3, Calb1, Aqp1, Snca
Axon extension	Biological process	Sema3d, Wnt5a, Epyc, Wnt3a, Bdnf, Ogn, Barhl2, Ntn1, Plxna4, Fmod, Nrp2, Slit3, Nkx6-1
Axon guidance	Biological process	Sema3d, Wnt5a, Epyc, Bmp7, Wnt3a, Bdnf, Ogn, Lhx1, Isl1, Ntn1, Atoh1, Otx2, Plxna4, Lhx9, Bmpr1b, Zic2, Lmx1a, Fmod, Robo2, Nrp2, Slit3, Foxd1
Spinal cord development	Biological process	Wnt1, Wnt3a, Lhx1, Isl1, Lhx5, Olig3, Lbx1, Dmrt3, Nkx6-1, Zic1

Pcdhα mutants possessed fewer myelinated axons

To assess the central nervous system myelination phenotype in Pcdhα knockout mice, hippocampal nerves of P21 Pcdhα-del and wild-type mice were examined using transmission electron microscopy. Strikingly, significantly fewer myelinated axons were observed in Pcdhα-del mice compared with the controls at a low magnification (**Figure 6A, B**). At high magnification, myelin sheaths around axons displayed alternately dark and bright lamellae, concentric configuration and consistent structural integrity in P21 wild-type mice. By contrast, myelin sheaths showed lamellar disorder, discrete appearance, and vacuoles in P21 Pcdhα-del mice (**Figure 6C, D**). Quantification revealed a significant decrease in the percentage of axonal myelination in mutants compared with wild-type mice (**Figure 6E**). These data demonstrated that Pcdhα is required for proper myelination at P21.

Discussion

An axon's main function is to transmit nerve impulses from the soma to other neurons or effector cells. During nervous system development, axons extend to a specific location to establish proper neural wiring with target cells (Ferreira and Paganoni, 2002; Scheiffele, 2003; Gibson and Ma, 2011; Chia et al., 2014). One theory to explain why adult central nervous system axons cannot regenerate after spinal cord injury is because of a nonpermissive environment in the extracellular matrix (Huang and Sheng, 2012; Li et al., 2016). A previous strategy indicated that axonal growth could be promoted by removing this extracellular inhibitory activity; however, recent studies revealed that this is insufficient. Increasing the intrinsic regenerative ability of adult neurons has emerged as a promising strategy after spinal cord injury (Hannila and Filbin, 2008; Smith et al., 2009). However, these findings only provide limited help and do not enable axons to achieve long-distance growth.

This study found that Pcdhα proteins may influence axon growth *in vivo* and that Pcdhα-del cultured hippocampal neurons exhibit a significant decrease in axonal length. In addition, *Pcdhα*-del mice exhibited a significant decrease in the degree of axon myelination *in vivo*. This is consistent with human genetic studies of a 5q31.3 microdeletion syndrome that causes delayed myelination in the human infant central nervous system (Shimojima et al., 2011). Our results show that the *Pcdhα* cluster is important for the growth and maturation of axons. Moreover, axonal expression of Pcdhα proteins is gradually repressed in mature mouse neurons (Morishita et al., 2004), indicating that the *Pcdhα* cluster may play a crucial role in axon development. RNA-Seq experiments demonstrated that genes related to axon extension and axon guidance, such as BDNF, Fmod, Nrp2, OGN, and Sema3d are down-regulated in the absence of Pcdhα. Many studies have shown that these genes participate in the growth of axons (Liu et al., 2004; Winckler, 2007; McIntyre et al., 2010; Steinhart et al., 2014; Taku et al., 2016; Guo et al., 2017).

In summary, the *Pcdhα* cluster functions in axon outgrowth and myelination. Neuron-intrinsic factors regulate axonal development in complex ways. Reactivating the expression of this gene can help repair adult mammalian spinal cord injury. This study focuses on morphological observations and does not clarify the mechanism by which the *Pcdhα* cluster influences axon outgrowth and myelination. Furthermore, the mechanism by which expression of the *Pcdhα* cluster is activated remains unclear, highlighting the need for additional strategies to reactivate intrinsic axonal growth after injury.

Author contributions: *QW and QS participated in study concept and design. WCL, YXZ and JZ performed experiments. WCL and PQ performed data analysis. WCL, QW, and QS wrote the paper. WCL was responsible for statistical analysis and experiments. All authors approved the final version of the paper.*
Conflicts of interest: *There are no conflicts of interest to declare.*
Financial support: *This study was supported by a grant from the Science and Technology Commission of Shanghai Municipality of China, No. 12441900702. The conception, design execution, and analysis of experiments, as well as the preparation of and decision to publish this manuscript, were made independent of this funding organization.*
Research ethics: *This study was approved by the Animal Ethics Committee, Shanghai Jiao Tong University, China (approval No. 1602029).*
Data sharing statement: *Datasets analyzed during the current study are available from the corresponding author on reasonable request.*
Plagiarism check: *Checked twice by iThenticate.*
Peer review: *Externally peer reviewed.*
Open access statement: *This is an open access article distributed under the terms of the Creative Commons Attribution-NonCommercial-ShareAlike 3.0 License, which allows others to remix, tweak, and build upon the work non-commercially, as long as the author is credited and the new creations are licensed under identical terms.*
Open peer reviewers: *Chun Liu, Michigan State University, USA; Jongmin Lee, Konkuk University, Korea.*

References

Abe N, Cavalli V (2008) Nerve injury signaling. Curr Opin Neurobiol 18:276-283.

Albertin CB, Simakov O, Mitros T, Wang ZY, Pungor JR, Edsinger-Gonzales E, Brenner S, Ragsdale CW, Rokhsar DS (2015) The octopus genome and the evolution of cephalopod neural and morphological novelties. Nature 524:220-224.

Beattie MS, Li Q, Bresnahan JC (2000) Cell death and plasticity after experimental spinal cord injury. Prog Brain Res 128:9-21.

Biswas S, Emond MR, Duy PQ, Hao le T, Beattie CE, Jontes JD (2014) Protocadherin-18b interacts with Nap1 to control motor axon growth and arborization in zebrafish. Mol Biol Cell 25:633-642.

Chen WV, Maniatis T (2013) Clustered protocadherins. Development 140:3297-3302.
Cheng PL, Poo MM (2012) Early events in axon/dendrite polarization. Annu Rev Neurosci 35:181-201.
Chia PH, Chen B, Li P, Rosen MK, Shen K (2014) Local F-actin network links synapse formation and axon branching. Cell 156:208-220.
Chilton JK (2006) Molecular mechanisms of axon guidance. Dev Biol 292:13-24.
Dickson BJ (2002) Molecular mechanisms of axon guidance. Science 298:1959-1964.
Fawcett JW (2006) Overcoming inhibition in the damaged spinal cord. J Neurotrauma 23:371-383.
Ferreira A, Paganoni S (2002) The formation of synapses in the central nervous system. Mol Neurobiol 26:69-79.
Filbin MT (2003) Myelin-associated inhibitors of axonal regeneration in the adult mammalian CNS. Nat Rev Neurosci 4:703-713.
Filbin MT (2008) PirB, a second receptor for the myelin inhibitors of axonal regeneration Nogo66, MAG, and OMgp: implications for regeneration in vivo. Neuron 60:740-742.
Fitch MT, Silver J (2008) CNS injury, glial scars, and inflammation: Inhibitory extracellular matrices and regeneration failure. Exp Neurol 209:294-301.
Gibson DA, Ma L (2011) Developmental regulation of axon branching in the vertebrate nervous system. Development 138:183-195.
Guo Y, Ma Y, Pan YL, Zheng SY, Wang JW, Huang GC (2017) Jisuikang, a Chinese herbal formula, increases neurotrophic factor expression and promotes the recovery of neurological function after spinal cord injury. Neural Regen Res 12:1519-1528.
Hannila SS, Filbin MT (2008) The role of cyclic AMP signaling in promoting axonal regeneration after spinal cord injury. Exp Neurol 209:321-332.
Hasegawa S, Hirabayashi T, Kondo T, Inoue K, Esumi S, Okayama A, Hamada S, Yagi T (2012) Constitutively expressed Protocadherin-alpha regulates the coalescence and elimination of homotypic olfactory axons through its cytoplasmic region. Front Mol Neurosci 5:97.
Hasegawa S, Hamada S, Kumode Y, Esumi S, Katori S, Fukuda E, Uchiyama Y, Hirabayashi T, Mombaerts P, Yagi T (2008) The protocadherin-alpha family is involved in axonal coalescence of olfactory sensory neurons into glomeruli of the olfactory bulb in mouse. Mol Cell Neurosci 38:66-79.
Hayashi S, Takeichi M (2015) Emerging roles of protocadherins: from self-avoidance to enhancement of motility. J Cell Sci 128:1455-1464.
Hayashi S, Inoue Y, Kiyonari H, Abe T, Misaki K, Moriguchi H, Tanaka Y, Takeichi M (2014) Protocadherin-17 mediates collective axon extension by recruiting actin regulator complexes to interaxonal contacts. Dev Cell 30:673-687.
Hu J, Selzer ME (2017) RhoA as a target to promote neuronal survival and axon regeneration. Neural Regen Res 12:525-528.
Huang K, Sheng WB (2012) Formation of glial scar in the rat spinal cord after injury. Zhongguo Zuzhi Gongcheng Yanjiu 16:3671-3674.
Imai T, Yamazaki T, Kobayakawa R, Kobayakawa K, Abe T, Suzuki M, Sakano H (2009) Pre-target axon sorting establishes the neural map topography. Science 325:585-590.
Kadoya K, Tsukada S, Lu P, Coppola G, Geschwind D, Filbin MT, Blesch A, Tuszynski MH (2009) Combined intrinsic and extrinsic neuronal mechanisms facilitate bridging axonal regeneration one year after spinal cord injury. Neuron 64:165-172.
Kim HS, Lee J, Lee DY, Kim YD, Kim JY, Lim HJ, Lim S, Cho YS (2017) Schwann cell precursors from human pluripotent stem cells as a potential therapeutic target for myelin repair. Stem Cell Reports 8:1714-1726.
Kim SY, Yasuda S, Tanaka H, Yamagata K, Kim H (2011) Non-clustered protocadherin. Cell Adh Migr 5:97-105.
Leung LC, Harris WA, Holt CE, Piper M (2015) NF-Protocadherin regulates retinal ganglion cell axon behaviour in the developing visual system. PLoS One 10:e0141290.
Li JF, Yan JY, Xia RF, Zhang X, Tan XH, Guan J, Ye Z, Zhang SL (2016) Glial scar formation and astrocyte role in spinal cord injury. Zhongguo Zuzhi Gongcheng Yanjiu 20:5609-5616.
Liu K, Tedeschi A, Park KK, He Z (2011) Neuronal intrinsic mechanisms of axon regeneration. Annu Rev Neurosci 34:131-152.
Liu Y, Berndt J, Su F, Tawarayama H, Shoji W, Kuwada JY, Halloran MC (2004) Semaphorin3D guides retinal axons along the dorsoventral axis of the tectum. J Neurosci 24:310-318.
Lu Y, Belin S, He Z (2014) Signaling regulations of neuronal regenerative ability. Curr Opin Neurobiol 27:135-142.
McAllister AK (2007) Dynamic aspects of CNS synapse formation. Annu Rev Neurosci 30:425-450.
McIntyre JC, Titlow WB, McClintock TS (2010) Axon growth and guidance genes identify nascent, immature, and mature olfactory sensory neurons. J Neurosci Res 88:3243-3256.
McKerracher L, Rosen KM (2015) MAG, myelin and overcoming growth inhibition in the CNS. Front Mol Neurosci 8:51.
Morishita H, Yagi T (2007) Protocadherin family: diversity, structure, and function. Curr Opin Cell Biol 19:584-592.
Morishita H, Kawaguchi M, Murata Y, Seiwa C, Hamada S, Asou H, Yagi T (2004) Myelination triggers local loss of axonal CNR/protocadherin alpha family protein expression. Eur J Neurosci 20:2843-2847.
Nathan FM, Li S (2017) Environmental cues determine the fate of astrocytes after spinal cord injury. Neural Regen Res 12:1964-1970.
Neumann S, Bradke F, Tessier-Lavigne M, Basbaum AI (2002) Regeneration of sensory axons within the injured spinal cord induced by intraganglionic cAMP elevation. Neuron 34:885-893.
Sánchez I, Hassinger L, Paskevich PA, Shine HD, Nixon RA (1996) Oligodendroglia regulate the regional expansion of axon caliber and local accumulation of neurofilaments during development independently of myelin formation. J Neurosci 16:5095-5105.
Scheiffele P (2003) Cell-cell signaling during synapse formation in the CNS. Annu Rev Neurosci 26:485-508.
Shimojima K, Isidor B, Le Caignec C, Kondo A, Sakata S, Ohno K, Yamamoto T (2011) A new microdeletion syndrome of 5q31.3 characterized by severe developmental delays, distinctive facial features, and delayed myelination. Am J Med Genet A 155A:732-736.
Smith PD, Sun F, Park KK, Cai B, Wang C, Kuwako K, Martinez-Carrasco I, Connolly L, He Z (2009) SOCS3 deletion promotes optic nerve regeneration in vivo. Neuron 64:617-623.
Steinhart MR, Cone-Kimball E, Nguyen C, Nguyen TD, Pease ME, Chakravarti S, Oglesby EN, Quigley HA (2014) Susceptibility to glaucoma damage related to age and connective tissue mutations in mice. Exp Eye Res 119:54-60.
Sun F, He Z (2010) Neuronal intrinsic barriers for axon regeneration in the adult CNS. Curr Opin Neurobiol 20:510-518.
Suo L, Lu H, Ying G, Capecchi MR, Wu Q (2012) Protocadherin clusters and cell adhesion kinase regulate dendrite complexity through Rho GTPase. J Mol Cell Biol 4:362-376.
Taku AA, Marcaccio CL, Ye W, Krause GJ, Raper JA (2016) Attractant and repellent cues cooperate in guiding a subset of olfactory sensory axons to a well-defined protoglomerular target. Development 143:123-132.
Truett GE, Heeger P, Mynatt RL, Truett AA, Walker JA, Warman ML (2000) Preparation of PCR-quality mouse genomic DNA with hot sodium hydroxide and tris (HotSHOT). BioTechniques 29:52, 54.
Winckler B (2007) BDNF instructs the kinase LKB1 to grow an axon. Cell 129:459-460.
Wu Q, Maniatis T (1999) A striking organization of a large family of human neural cadherin-like cell adhesion genes. Cell 97:779-790.
Wu Q, Zhang T, Cheng JF, Kim Y, Grimwood J, Schmutz J, Dickson M, Noonan JP, Zhang MQ, Myers RM, Maniatis T (2001) Comparative DNA sequence analysis of mouse and human protocadherin gene clusters. Genome Res 11:389-404.
Wu S, Ying G, Wu Q, Capecchi MR (2007) Toward simpler and faster genome-wide mutagenesis in mice. Nat Genet 39:922-930.
Wu S, Ying G, Wu Q, Capecchi MR (2008) A protocol for constructing gene targeting vectors: generating knockout mice for the cadherin family and beyond. Nat Protoc 3:1056-1076.
Xu Y, Du S, Yu X, Han X, Hou J, Guo H (2014) Human bone marrow mesenchymal stem cell transplantation attenuates axonal injury in stroke rats. Neural Regen Res 9:2053-2058.
Yagi T, Takeichi M (2000) Cadherin superfamily genes: functions, genomic organization, and neurologic diversity. Genes Dev 14:1169-1180.
Yang P, Yang Z (2012) Enhancing intrinsic growth capacity promotes adult CNS regeneration. J Neurol Sci 312:1-6.
Yang P, Wen HZ, Zhang JH (2010) Expression of a dominant-negative Rho-kinase promotes neurite outgrowth in a microenvironment mimicking injured central nervous system. Acta Pharmacol Sin 31:531-539.
Yiu G, He Z (2006) Glial inhibition of CNS axon regeneration. Nat Rev Neurosci 7:617-627.
Yu Y, Suo L, Wu Q (2012) Protocadherin alpha gene cluster is required for myelination and oligodendrocyte development. Dongwuxue Yanjiu 33:362-366.
Zipursky SL, Sanes JR (2010) Chemoaffinity revisited: dscams, protocadherins, and neural circuit assembly. Cell 143:343-353.

(*Copyedited by Yu J, Li CH, Qiu Y, Song LP, Zhao M*)